

Detection of a deep 3- μm absorption feature in the spectrum of Amalthea (JV)

Naruhisa Takato, Schelte J. Bus, Hiroshi Terada, Tae-Soo Pyo, Naoto Kobayashi

Supporting Online Materials

Surface contamination from Io

The optical reflectance spectrum contains little information about the bulk composition of Amalthea because of surface contamination from Io and alteration (i.e. space weathering) by heavy bombardment of micrometeorites and impacts of charged particles accelerated in Jupiter's strong magnetic field (*1*). However, for wavelengths longward of 0.8 μm , contamination by Io's ejecta does not interfere with the interpretation of the surface composition, because there is no strong absorption due to sulfur in the 0.8–4.2 μm wavelength range (*2, 3*). Only the blue absorption edge observed in Io's reflectance spectrum was seen in our spectra of Amalthea and Thebe shortward of 0.6 μm (Fig. S2 and (*4*)).

Space weathering of hydrous minerals

A recent laboratory experiment shows that space weathering can dehydrate the hydrous minerals (*5*). A possible explanation for the survival of the 3- μm absorption feature against such space weathering is that the impact of micrometeorites sandblast the surface of Amalthea faster than the surface can mature. Because the radius of the Hill sphere for Amalthea, the approximate limit to Amalthea's gravitational dominance, is about 1/400 that of a heliocentric asteroid with the same mass at 5 AU from the sun, the amount of the ejecta reaccumulated on Amalthea might be smaller than that on the asteroid. Micrometeorites erode the surfaces of the inner jovian satellites at a rate of $\sim 0.1 \mu\text{m year}^{-1}$, corresponding to a surface erosion of ~ 400 m over the age of solar system (*6*).

Spectral range of C, P, and D-type asteroid

Spectral ranges are defined by the following asteroids (*7–9*). D-type: asteroid number 152, 336, 368, 624, 773, 1143, 1867. P-type: 65, 76, 153, 476, 617. C-type: 10, 31, 86, 145, 356, 511, 521, 702, 772.

Table S1. Observation logs for Amalthea and Thebe. For spectroscopy, IRCS was used with its grism mode in 2.8–4.2 μm , and SpeX prism mode was used in 0.8–2.5 μm . The actual spectral resolution obtained by IRCS was 0.012 μm estimated by telluric absorption features. The spectral resolution obtained in our SpeX observation was $\sim 0.017 \mu\text{m}$. The objects were observed near their eastern or western elongations, and the position angles of the slit were set to about perpendicular to the Jupiter’s equatorial plane to avoid the change of the sky background between two dithering positions on the slit. Ephemerides of the satellites are calculated using JPL’s HORIZONS system (<http://ssd.jpl.nasa.gov/horizons.html>).

object	L/T^c	wavelength (μm)	Inst.	date (UT)	time	airmass	sky condition	exp. (sec)	slit width('')	ϕ^b ($^\circ$)	sub-earth Lon. ($^\circ$) Lat.	sub-solar Lon. ($^\circ$) Lat.	r^c (AU)	Δ^d (AU)
spectroscopy														
Amalthea	T	2.8–4.2	IRCS	Dec. 13, 2002	15:18 – 15:45	1.04 – 1.07	clear	720	0.9	8.9	311	0.8	2.0	4.689
Amalthea	T	2.8–4.2	IRCS	Feb. 19, 2003	08:48 – 08:55	1.01	clear	180	0.9	3.5	300	8.0	0.1	4.376
Amalthea	T	0.8–2.5	SpeX	Feb. 17, 2004	12:28 – 13:30	1.04 – 1.16	clear	3360	0.8	3.2	266	-4.8	-3.6	4.465
Thebe	T	0.8–2.5	SpeX	Feb. 17, 2004	13:44 – 14:03	1.18 – 1.31	clear	1920	0.8	3.2	273	-4.9	-4.2	4.465
Io	T	2.8–4.2	IRCS	Dec. 10, 2002	14:45 – 14:51	1.01	thin cirrus	240	0.9	9.2	286	0.1	0.5	4.730
HD63435 (G2III)		2.8–4.2	IRCS	Dec. 10, 2002	13:08 – 13:11	1.04	thin cirrus	80	0.9					
HD81809 (G2V)		2.8–4.2	IRCS	Dec. 13, 2002	16:13	1.26	clear	8	0.9					
HD81809 (G2V)		2.8–4.2	IRCS	Feb. 19, 2003	09:23	1.12	clear	40	0.9					
4 stars ^e		0.8–2.5	SpeX	Feb. 17 – 18, 2004	–	1.06–1.08	clear	–	0.8					
photometry														
Amalthea ^f	T	K	IRCS	Dec. 13, 2002	15:04	1.02	clear	10		8.9	299	0.8	308	4.689
Amalthea	L	J	IRCS	Nov. 02, 2003	15:33	1.44	clear	60		8.8	56	-3.4	65	5.876
Amalthea	L	H	IRCS	Nov. 02, 2003	15:45	1.37	clear	20		8.8	62	-3.4	71	5.876
Amalthea	L	K	IRCS	Nov. 02, 2003	15:55	1.32	clear	50		8.8	67	-3.4	76	5.875
Amalthea	T	K	IRCS	Dec. 27, 2003	16:15	1.06	clear	5		10.0	220	-6.6	230	5.037
Amalthea	T	L'	IRCS	Dec. 27, 2003	16:21	1.07	clear	225		10.0	223	-6.6	233	5.037
FS10 ^g		J	IRCS	Nov. 02, 2003	13:47	1.32	clear	120						
FS10		H	IRCS	Nov. 02, 2003	13:53	1.35	clear	150						
FS10		K	IRCS	Nov. 02, 2003	14:26	1.52	clear	150						
HD106965 ^h		K	IRCS	Dec. 27, 2003	16:27	1.05	clear	1.5						
HD106965		L'	IRCS	Dec. 27, 2003	16:31	1.06	clear	25						

(a) leading side (L) / trailing side (T)

(b) phase angle (sun – object – observer angle)

(c) heliocentric distance

(d) geocentric distance

(e) SA102-1081, SA105-56, SA107-998, and SA107-684

(f) A photometric standard star was not observed in this night. To determine the K-band magnitude, we used instrumental magnitude zeropoint, which is stable within 6 % during Oct. 2001 to Dec. 2003.

(g) UKIRT faint standard star: $K = 14.987$, $J - H = -0.100$, $H - K = -0.142$ (DA2)

(h) UKIRT bright standard star: $K = 7.316$, $L' = 7.34$ (A2)

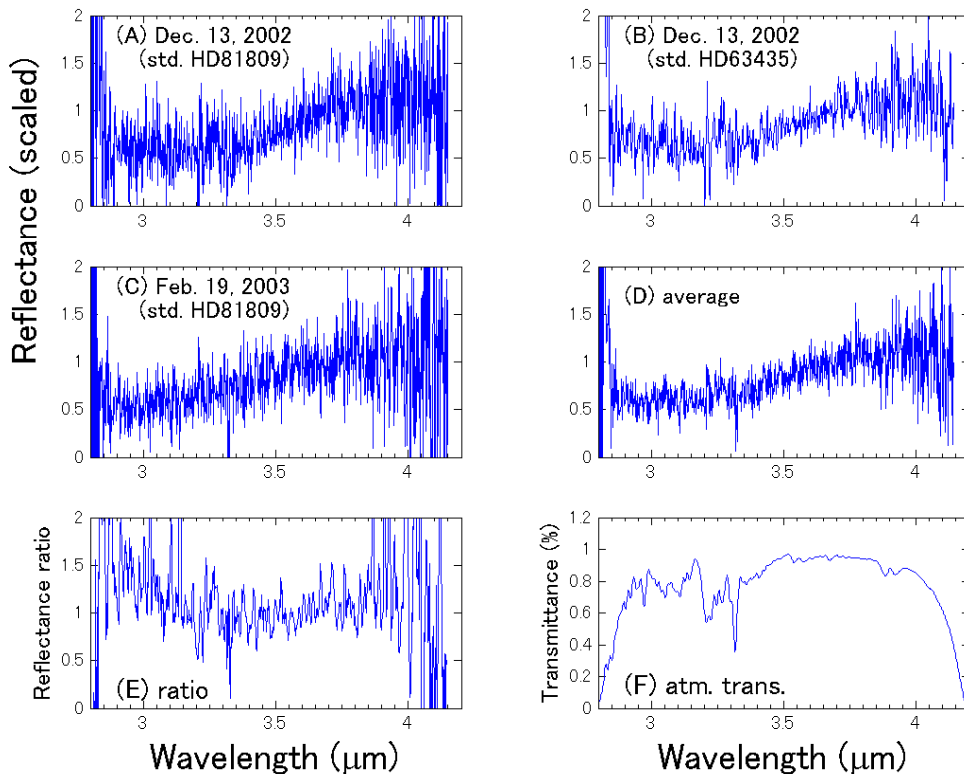


Figure S1. Reliability of the 2.8–4.2 μm spectra of Amalthea. **(A)** Reflectance spectrum obtained on Dec. 13, 2002 by dividing by the spectrum of a solar analog star HD81809 (G2V) whose telluric features were scaled to the airmass at the Amalthea observation. **(B)** The same as (A) but HD63435 (G2III) was used as a solar analog star. The atmospheric absorptions of Amalthea and HD63435 were corrected with the ATRAN software package (11). **(C)** Reflectance spectrum obtained on Feb. 19, 2003 by dividing by the spectra of HD81809 observed in the same night. **(D)** Weighted average of (A), (B) and (C). **(E)** Ratio of the two reflectance spectra obtained on Dec. 13, 2002 and Feb. 19, 2003 (5-pixel smoothing is applied). **(F)** An example of atmospheric transmission curve calculated using the ATRAN convolved to the observing spectral resolution. The difference between the two Amalthea spectra divided by different standard stars is negligibly small ((A) and (B)). The difference between the spectra obtained in the two different observing nights is seen at wavelengths shortward of 3.1 μm (E), and the difference is about 30 % at 3.0 μm . This difference is due to incomplete atmospheric absorption corrections. A small bump at 3.2–3.3 μm is also due to incomplete atmospheric corrections. No correction for the thermal emission from Amalthea is applied because of its low surface temperature of ~ 164 K (10). (The thermal emission is less than 1 % of the reflected light.)

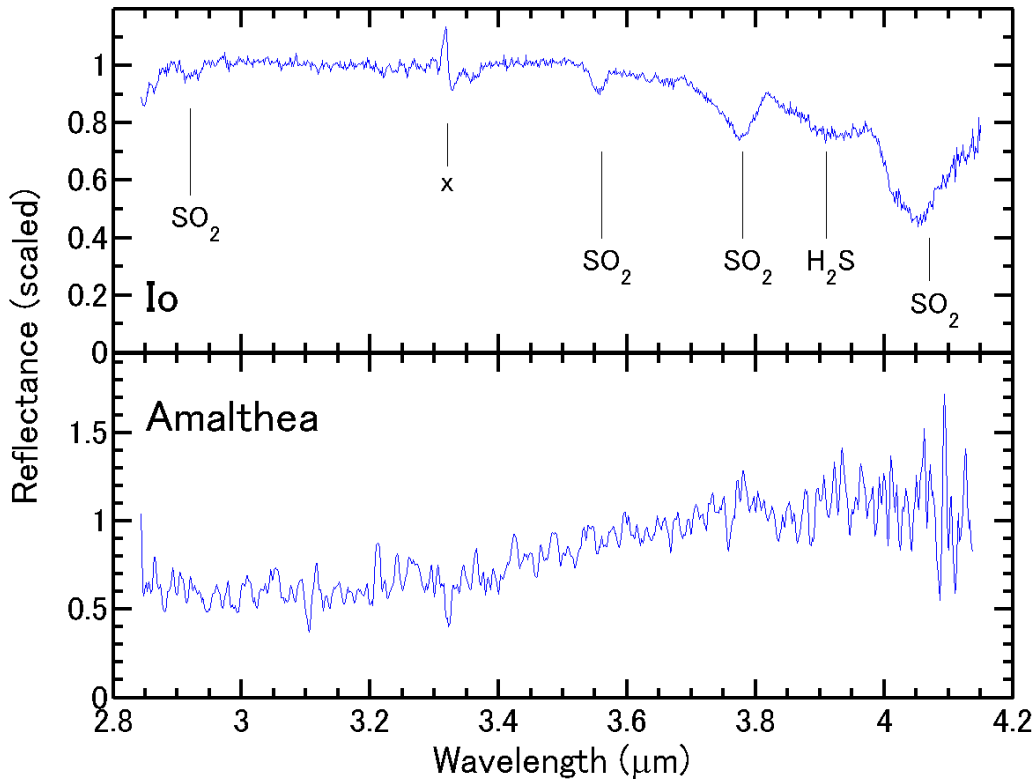


Figure S2. A spectral comparison of Amalthea with Io. The spectrum of Io (observed on Dec. 10, 2002) exhibits several absorption bands attributed to SO_2 and H_2S , while those absorptions are not detected in the Amalthea's spectrum. A mark "x" denotes incomplete correction of a telluric band. Band assignments in Io's spectrum are taken from Nash and Betts 1998 (12).

References:

1. J. Gradie, P. Thomas, J. Veverka, *Icarus* **44**, 373 (1980).
2. D. B. Nash, *Appl. Opt.* **25**, 2427 (1986).
3. K. A. Fuller, H. D. Downing, M. R. Query, in *Handbook of Optical Constants of Solids III*, E. D. Palik, Ed. (Academic Press, San Diego, 1998), pp. 899–922.
4. D. B. Nash, B. H. Betts, in *Solar System Ices*, B. Schmitt, C. de Bergh, M. Festou, Eds. (Kluwer, Netherlands, 1998), pp. 607–637.
5. T. Hiroi, L. V. Moroz, T. V. Shingareva, A. T. Basilevsky, C. M. Pieters, *34th LPI*, #1324 (2003).
6. J. A. Burns *et al.*, *Science* **284**, 1146 (1999).
7. B. Zellner, D. J. Tholen, E. F. Tedesco, *Icarus* **61**, 355 (1985).

8. J. F. Bell, P. D. Owensby, B. R. Hawke, M. J. Gaffey, *Lunar Planet. Sci.* **19**, 57 (1989).
9. A. Kanno *et al.*, *Geophys. Res. Let.* **30**, 1909 (2003).
10. D. P. Simonelli, *Icarus* **54**, 524 (1983).
11. S. D. Lord, “A new software tool for computing earth’s atmospheric transmission of near- and far-infrared radiation” (NASA TM-103957, NASA Ames Research Center, Moffett Field, 1992).
12. D. B. Nash, B. H. Betts, in *Solar System Ices*, B. Schmitt, C. de Bergh, M. Festou, Eds. (Kluwer, Dordrecht, 1998), pp. 607–637.